Teaching geometric modeling algorithms and data structures through laser scanner acquisition pipeline

Stefka Gueorguieva, Remi Synave, Christine Couture

Teaching geometric modeling algorithms and data structures through laser scanner acquisition pipeline

Gueorguieva S.†, Synave R†. and Couture-Veschambre,Ch.‡

†UMR5800, Laboratoire Bordelais de Recherche en Informatique,
‡UMR5199 PACEA, Laboratoire d'Anthropologie des Populations du Passé,
Université Bordeaux1, France

Abstract. Experiences from geometric modeling course based on a specific teaching medium, namely trochlear surface reconstruction from laser scans, its evaluation in terms of shape feature measurements and finally its instantiation through 3D printing, are presented. Laser scanner acquisition, reconstruction and 3D printing lend well to teaching general concepts in geometric modeling for several reasons. First, starting and ending with real physical 3D objects (the talus and its 3D print) provide in addition to the classical visual feedback a material feedback for correctness of treatments all over the pipeline. Second, the notion of error during each step of the pipeline is illustrated in a very intuitive way through length measurements, manual ones with calipers on the tali, and numerical ones with arc and chord lengths on the numerical reconstructions. Third, students are involved with challenging scientific problems and produce semester-long projects included in larger scaled project of cultural heritage preservation. Our believe is that this approach gives a deeper understanding of both theoretical and application issues in geometric modeling.

Keywords: *geometric modeling, digital paleoanthropology, cultural heritage preservation, laser scanner acquisition, image registration, image reconstruction, 3D printing*

1 Introduction

Geometric modeling evolves into a great variety of visual computing applications as 3D shape matching and recognition [1, 2], medical image analysis [3] and cultural heritage preservation [4–8]. Geometric models capture spatial aspects of the objects of interest for an application [9–11] and necessitate rigor mathematical foundations [12–18].

Unfortunately, the mathematical prerequisites are often unappealing to college students and the visual representation of 3D objects is usually considered as a final goal. Often, facet (planar face) models correspond to "soup" of polygons with degenerate polygons, holes and self-intersecting faces. Such models could be acceptable for rough graphical representation but when looking for surface feature estimation as the surface normal for example, these models lead to erroneous calculation. A possible way to handle such irregularities is to locate artefacts through geometric intersection tests [19, 20], to refine the underlying mesh in singular points and then to produce a manifold surface subdivision. These treatment is a commonly employed operation when integrating different scan views in a laser scanner acquisition based surface reconstruction. The advantage in making use of the laser scanner acquisition pipeline is that theoretical notions as $r - sets$ and $3D\ manifolds$, topological invariants and Euler characteristics, have an imminent impact in the results. Another example of geometric model prevailing property is the validity to argue if the model corresponds to (at least) one object. In the terms of the three level hierarchical view of modeling [11, 21], "physical object $\rightarrow$ mathematical models of objects $\rightarrow$ representations of objects", a valid geometric model could correspond to a mathematical model but not to a physical object. A new intuition on validity is brought to an active state through the 3D printing. The pipeline supports a three level graph view, "physical object $\leftrightarrow$ mathematical models of objects $\leftrightarrow$ representations of objects". Once the object boundary surface is reconstructed, a STL file [22] could be produced and a synthetic physical object reproduction, a 3D print, could be output. The distinction between valid and "printable" geometric model allows to close up the cycle "physical object ↔ mathematical models of objects ↔ representations of objects ↔ physical object". Each level of these modeling view is clearly identified through the pipeline and practitioner students can themselves evaluate the quality of all intermediate results and the final product. The control is done through manual measurements on the physical supports (bone specimen or its 3D print) and through numerical measurements on the numerical object reconstruction. The purpose of the present research is to show our experience in how to teach the algorithms and data structures underlying the pipeline. Our objective is to emphasize the practice interest of geometric modeling theoretical foundations for both computation implementation and anthropology investigations. Our believe is that this approach will engage students in learning geometric modeling through the development of solutions to scientific relevant problems. In the following, the main steps are explicated with the corresponding accompanying references. This program is proposed as a MS degree course of geometric modeling in the Department of Computer Science at the University of Bordeaux 1. Examples of the student project final results are also provided.

2 Laser scanner acquisition, registration and integration

There are several examples of 3D model acquisition pipelines [23, 4, 5, 7, 24–26]. In our case, the acquisition is done by a non-contact 3D digitizer VIVID 300/VI-300 with a laser wavelength $\lambda = 690nm$ and maximal optical power $P\_Max = 7mW$, object length range is in the limits of $[0.55m, 1.2m]$, field of view is in the limits of $[185mm, 395mm]$ and output data points 400×400. An illustration of talus acquisition with VIVID 300/VI-300 and Polygon Editing Tool is given in Fig. 1. Two views of the talus in Fig. 1(left) are registered in Fig. 1(center). It should be noted that the rough acquisition for a view corresponds to the mesh model shown in Fig. 2. The human operator is supposed to clean up those parts that are out of the region of interest and to produce the model given in Fig. 1(left). The final step is the integration of all scans and bringing forward for consideration the reconstructed surface as shown in Fig. 1(right). Acting with the system for a short time is sufficient to identify crucial points as:

- The optimal values for the laser power (% of P_Max ?) and the object distance.
  A few protocols including technical data sheets for the laser scanner measurements are known [27].
- The initial alignment and the partial overlap between sequential scans.
  The widely used in range image registration Iterative Closest Point(ICP) algorithm and its derivatives [28–33] strongly depend on both characteristics.
- The extent and the constraints to interpolate and/or approximate cloud points during the integration.
  Using Polygon Editing Tool for example, one can easily observe surface artefacts as undesired smoothing and lost of details in the reconstructed surface.

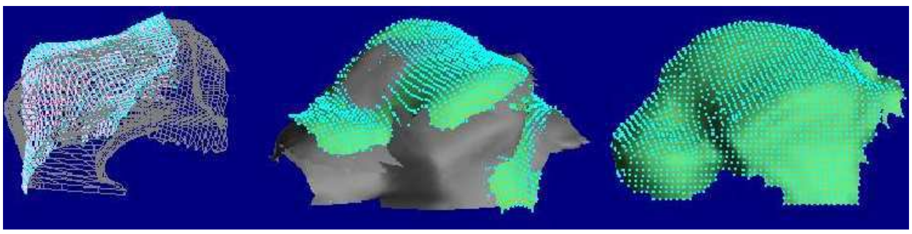

Fig. 1. Polygon Editing Tool: (left) Two scans (center) Scan registration (right) Scan integration

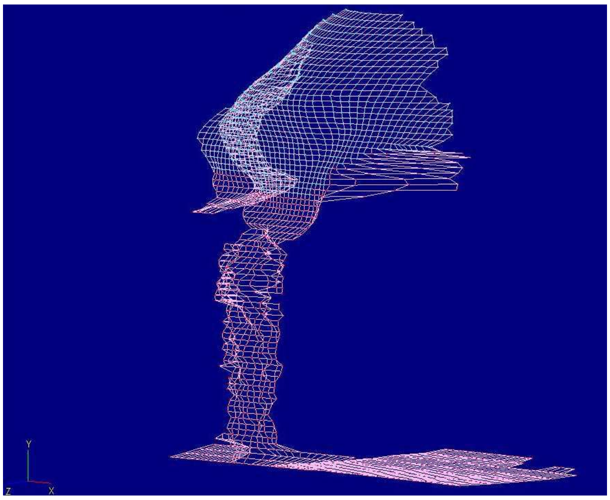

Fig. 2. Polygon Editing Tool: erroneous acquisition

Along this first stage in the training program, students are mostly supposed to act as final users of industrial software. As long as such softwares are "black boxes" no technical details are provided and thus personal investigations are encouraged in parallel with an introductionary course in geometric modeling fundamentals.

3 Object boundary reconstruction and evaluation

3.1 Programming projet

At this period, students start with a programming project dealing with surface reconstruction from 3D range images [34–36] obtained through the first stage. The range images could represent individual or integrated views of the studied objects and the goal is to construct valid surface mesh models.
The following requirements are implied:

- The data structures in used [37] should support:
  1. Efficient topological queries as variable sized vertex neighbourhood construction referring to the quad-edge [38], the winged-edge [39, 40] or the half-edge [41] data structures.
  2. Evaluated boundary representation for rapid visualisation.
- The models should fulfil mesh element quality criteria [42–45] and geometric cohererence of data [46, 47].

In order to broach the geometric computations students are urged to experiment with examples of robustness problems [48–52] and in particular the *Core* [53, 54] and *LEDA* [55] libraries. Along with geometric intersection tests essential in quality mesh improvement, a set of mesh query based operations are also required:

- Calculation of Euler characteristics of the underlying object boundary surface [56–58].
- Geodesic path construction between a pair of source and destination vertices [59–68].

Finally, as an optional functionality, the discrete curvature estimation [69–72] at mesh model vertices is required. This feature is helpful to indicate the characteristic vertex corresponding to chosen landmark as long as it is often situated either on spherical or hyperbolic point. In case when this functionality is not implemented the choice is made by visual appreciation.

These programming projects are developed as a collaborative work within two or three person team. Weekly, each team present the advancement of the project. The implementation is done in $C++$ using either $Qt4$ or GTK graphical user interface[73, 74].

3.2 Validation

Once the student software becomes operating the validation of the boundary surface reconstruction starts with geometric features evaluation. First, manually on the studied specimen and then by simulating the same measurements on the numerical representation.

For our experience we study osteological specimens issued from an archaeological series emerging from the "Soeurs Grises"'s cemetery (medieval sample, XV-XVIII° century) located in Beauvais (Oise, France). In particular we are interested in the (trochlear) articular facet on the superior surface of the talus's body involved in the ankle joint and consequently in the foot position during locomotion [75]. An illustration is given in Fig. 3.

Fig. 3. Left talus: (a) Superior view (b) Anatomical position (c) 3D print

Three pairs of landmark points for the trochlear shape are defined following [76–78]: $(P_{apmr}, P_{aplr}), (P_{ipmr}, P_{iplr})$ and (P_{ppmr}, P_{pplr}). Each pair corresponds to one position: the anterior, the intermediate and the posterior with respect to the frontal plan. A point of the pair is either on the medial or on the lateral process of the trochlea with respect to the sagittal plane, denoted as medial or lateral ridge as illustrated in Fig. 4. Anthropometric chord and arc length mesurements are performed manually with caliper and millimetre ruler band on the specimens.

For the validation of the trochlear surface reconstruction each manual measurement is replicated on the mesh model. Chord measurements are similar to euclidean distances between the pair of characteristic vertices, each one corresponding to an anatomical landmark point. Arc measurements agree with geodesic distances between the characteristic vertices. Statistical analysis [79] is performed over all samples in order to evaluate the range interval for the standard deviations for the measured entities. All results are presented and appreciated by an expert in the application field namely an anthropologist. According to our experience these discussions are particularly fruitful as long as the visual and the numerical feedback of the trochlear surface reconstruction are

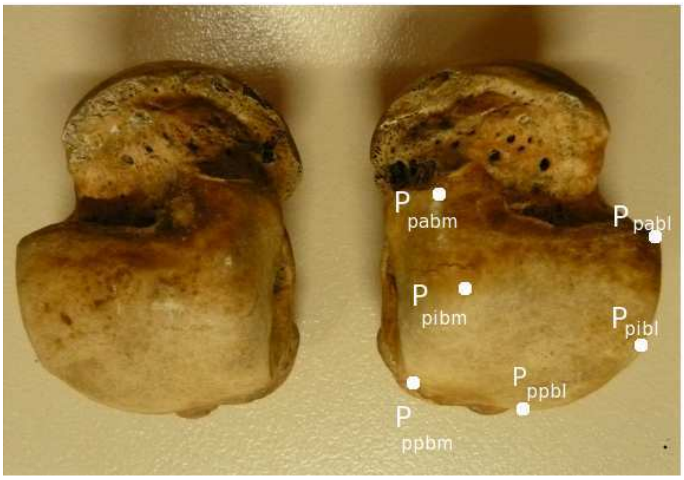

Fig. 4. Anatomical landmark points on the trochlear surface.

commented by a potential final user of such kind of software package. In this way the developer is also confrontated with the technical trade specifications.

4 Offsetting object boundary and 3D printing

Creating of 3D print models becomes very popular as research and training tool [80–83]. The 3D printer put to student's disposal is an Objet Eden250 3D printing system. The input of the 3D printing system is the STL format [22] that does not guaranty the correctness of the underlying surface namely to correspond to an oriented 2D manifold without boundaries. The result of the reconstruction on the previous stage is a triangulated surface but with possible existing boundaries as for example when the object boundary is partially reconstructed and does not enclose a bounded volume (shell surface). For such cases initial surface should be offset [84–89]. The offset direction is chosen opposite to the normal direction in order to preserve the chord and arc metric of the initial shell surface. The offsetting and the STL output are added as new functionalities to the programming project. Finaly, each student team produces and evaluates the 3D print of the studied talus specimen. Evaluating the precision of the complete pipeline from the acquisition through the reconstruction to the 3D printing is an innovative approach to validate the whole treatment channel and the supported data structure and algorithm implementations. A few similar works are known related to vision system based on computed tomography and commercial software [90]. According to the technical specifications the typical tolerance of Eden250 is of $0.1mm$. The student experimental results show that the variance of manual measurements on the 3D print is similar to the one of manual measurements on the original specimen but that the absolute values of chord and arc lengths increase for the 3D print. It is observed that the interchangeability of both supports is limited to a resolution of $1.5mm$.

5 Discussion and experimental results

The elaborated training program is successfully applied as a graduated course in the master of Computer Science at the University of Bordeaux 1. It should be noticed that mathematical prerequisites and namely notions from algebraic topology of surfaces and differential geometry are difficult to apprehend as long as in the previous Computer Science degree courses students do not broach these subjects. Often, problems are identified but the mathematical apparatus to resolve them takes too long time to become familiar with enough in order to be used. Dealing with the

laser acquisition pipeline as a whole permits to remain flexible with respect to the pedagogical objectives that can be adapted according to individual skills of the members in a programming project team.
For the basic pipeline processing steps:
registration, reconstruction, offsetting, geodesic path computation and curvature estimation, rough algorithms are proposed as initial guess to be improved as students go along. See for example, in Fig. 5(b) the illustration of the shortest path calculation between the source (P_{pabl}) and the destination (P_{ppbl}) characterstic vertices. The rough algorithm is the Dijkstra algorithm. Very quickly a shortest path computation could be implemented and visualized but the limits of a naive implementation are obvious even for mesh models with a total number of vertices under the range of 10^4. Further, the problem of non-uniqueness of the shortest path and the lack of a measurement direction as in physical measurements with caliper or millimetre ruler band could be seen in Fig. 5(a). Finally, the choice of the path extremity in a specified mesh vertex position could be tedious and erroneous task so that the possibility of interaction with vertices in a variable sized neighborhood of source (destination) vertex is useful as shown in Fig. 5(c).

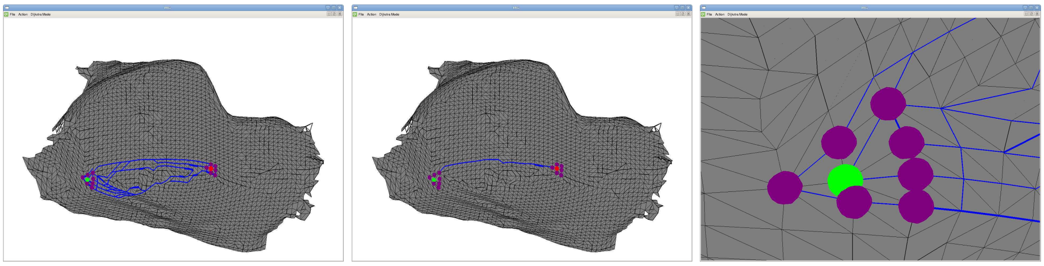

(a) (b) (c)

Fig. 5. M. Fichoux and D. Sabary's programming project : geodesic path calculation.

The offsetting of a mesh model from Fig. 6(a) is illustrated in Fig. 6(b) and Fig. 6(c). The rough algorithm consists in a vertex based translational extrusion. As long as for 3D printing of shell surface we need a narrowly banded extruded surface, the offset vector is of small magnitude and in almost all tested models self-intersections are avoided.

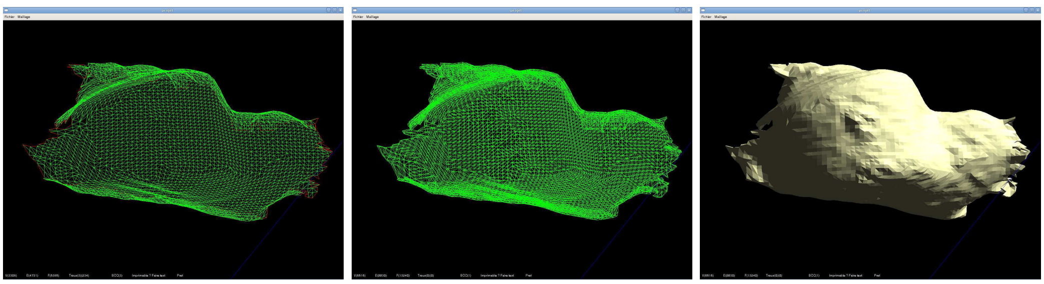

(a) (b) (c)

Fig. 6. Ch. Mary and Ch. Delmotte's programming project : offsetting for 3D printing.

According to our experience discrete curvature evaluation stands up as one of the most apprehended problem. Starting with [70] and the *GSL* GNU Scientific library for matrix operations, an initial evaluation could be reported as shown in Fig. 7 where flat like regions are displayed in blue color and the curved ones in different graduations of the green color.

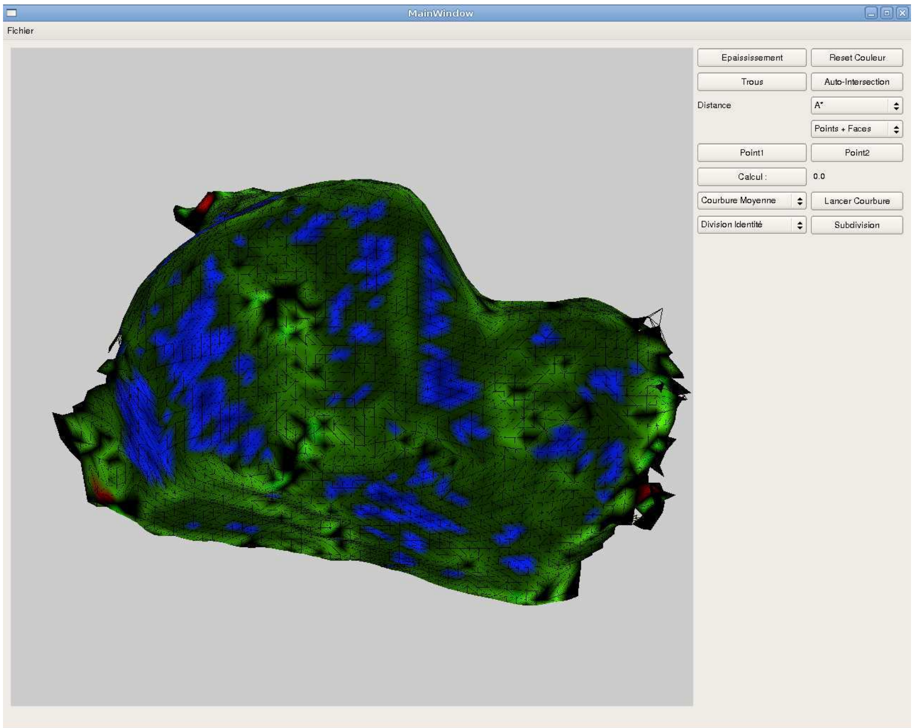

Fig. 7. J. Laviole and R. Leguay's programming project : discrete surface curvature evaluation.

There are two check on points for the developed software:
First, evaluate the reconstructed object boundary in terms of chord and arc measurements between characteristic vertices on the underlying mesh model, and second, estimate the same geometric features on the corresponding 3D print. The computed values are compared with the manual measurements on the original specimen. The goal is to establish the degree of interchangeability along the different object reproductions, the numerical representations and/or the synthetic ones. The results are summed up for the specimen the BCT92-S319-G in Fig. 8(a) for the original individual, in Fig. 8(b) for the reconstruction, and in Fig. 8(c) for the 3D print. By analogy, in Fig. 9(a), Fig. 9(b) and Fig. 9(c) the measurements on BCT92-S380-G are detailed. In each figure, on the left side, computed values are provided. The notations in use are as follows:

1. The length of the trochlea, M4, is the length of the chord joining the crossing points of the anterior and the posterior ridges with the medial lengthwise curvature of the trochlea.
2. The width of the trochlea, M5, is the length of the chord $P_{ipmr}P_{iplr}$ joining the medial and the lateral ridges.
3. The posterior width of the trochlea, M5(1), is the length of the chord $P_{ppmr}P_{pplr}$ joining the medial and the lateral ridges.
4. The anterior width of the trochlea, M5(2), is the length of the chord $P_{apmr}P_{aplr}$ joining the medial and the lateral ridges.
5. The medial chord of the trochlea, Cm, is the chord length between $P_{ppmr}P_{apmr}$.
6. The lateral chord of the trochlea, Cl, is the chord length between $P_{pplr}P_{aplr}$.
7. The medial arc of the trochlea, Am, is the length of the curve joining P_{ppmr} and P_{apmr} along the medial ridge.
8. The lateral arc of the trochlea, Al, is the length of the curve joining P_{pplr} and P_{aplr} along the lateral ridge.

These chord and arc measurements provide the support for the morphometric analysis performed at the reconstruction and the prototyping stage of talus repository reproduction.

On the right side in the figures, the standard deviation distribution for the sampled values is shown.

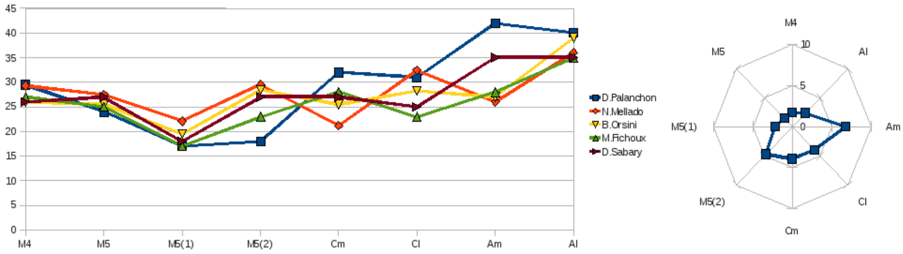

(a)

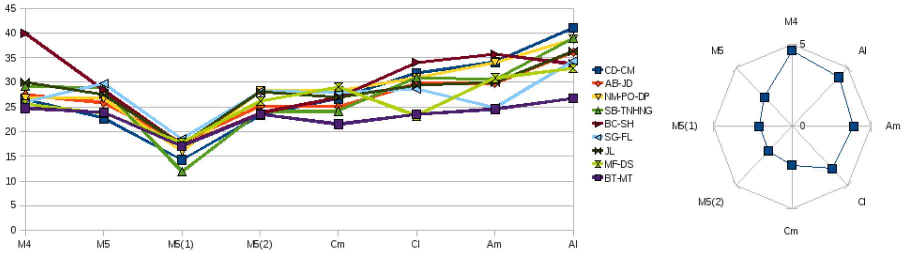

(b)

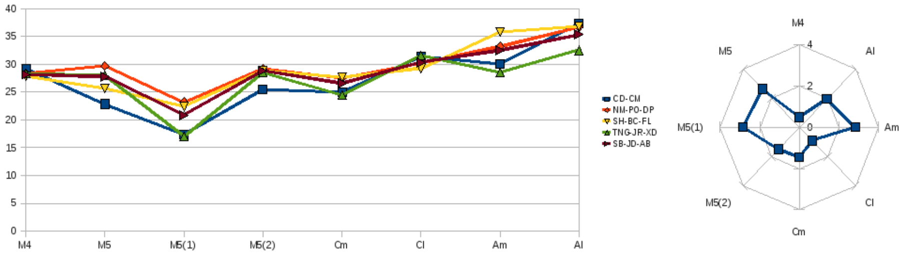

(c)

Fig. 8. Chord and arc measurements on BCT92-S319-G: (a) Original specimen (b) Numerical reconstruction (c) 3D print

It could be seen that range intervals of the standard deviations decrease for measurements on the 3D prints. In fact, evaluate original specimen with partially damaged ridges is subjective depending on the human operator interpretation. While, after the reconstruction, the corresponding parts on the boundary are "repaired" and thus the positioning of the characterictic vertices is less uncertain. Moreover, range intervals of the chord and arc lengths on the tali tend to increase for their counterparts on the 3D prints in average with $1.5mm$. On the contrary, length estimations on numerical models oscillate around manually measured values within $1mm$ absolute value interval. One can conclude that the dominant of the error in the pipeline occurs during the reconstruction and consequently further improvement should be supplied.

6 Conclusion

The present work relates our experiences in teaching geometric modeling fundamentals through the laser scanner acquisition based pipeline and with a particular application domain of cultural heritage preservation. We choose to cover the pipeline as a whole starting with the original specimen, scanning, registrating and reconstructing the object boundary, and finally, printing it. The major advantage of this approach is that in addition to the classical visual feedback in the visual systems, a material feedback is also produced and in this way the correctness of treatments all over the pipeline is evaluated. The notion of error is illustrated in a very intuitive way through length measurements: manual ones with calipers and millimetre ruler band on the tali and their 3D prints, and numerical ones on the numerical reconstructions. All over the covered subjects, students are involved with challenging scientific problems looking for efficient computation solutions. Our believe is that this approach gives a deeper understanding of both theoretical and application issues in geometric modeling.

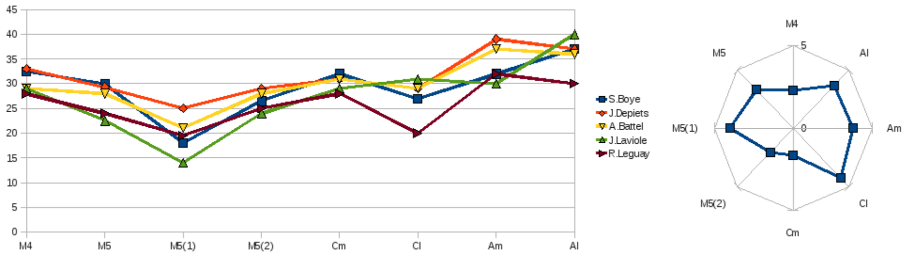

(a)

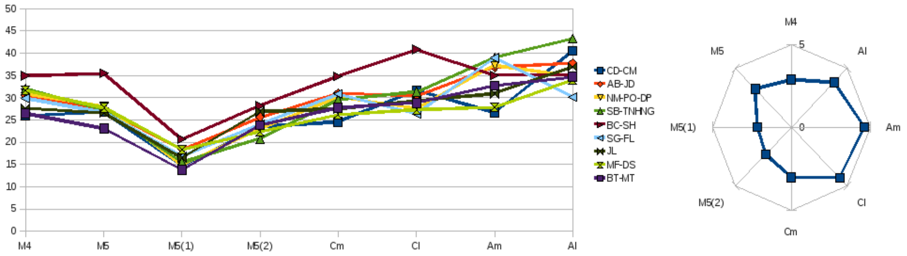

(b)

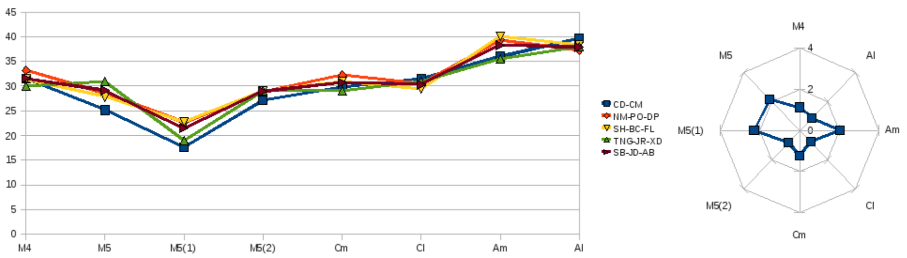

(c)

Fig. 9. Chord and arc measurements on BCT92-S380-G: (a) Original specimen (b) Numerical reconstruction (c) 3D print

Aknowledgements This work was supported by our student classes during the autumn semester of the years 2008-09 and 2009-10, and with a particular contribution of Ch. Delmotte, Ch. Mary, N. Mellado, B. Orsini, D. Palanchon, S. Boye, T.N.H. N'Guyen, J. Laviole, G. Simon, F. Lepretre, S. Damien, M. Fichoux, B. Tricoire and M. Troale.
The authors wish to thank Mr. Patrice Courtaud for providing the collection from Pessac osteological repository, and Mr. J.-M. Femolan in charge of the complete collection from Archaelogical Department of Beauvais city concil.

References

1. Belongie, S., Malik, J., Puzicha, J.: Shape matching and object recognition using shape contexts. IEEE Trans. Pattern Anal. Mach. Intell. **24** (2002) 509–522
2. Mori, G., Belongie, S.J., Malik, J.: Efficient shape matching using shape contexts. IEEE Trans. Pattern Anal. Mach. Intell. **27** (2005) 1832–1837
3. Ayache, N.: Epidaure: A research project in medical image analysis, simulation and robotics at inria. IEEE Trans. Med. Imaging **22** (2003) 1185–1201
4. Levoy, M.: The digital michelangelo project. In: 3DIM. (1999) 2–13
5. Bernardini, F., Rushmeier, H.E.: The 3d model acquisition pipeline. Comput. Graph. Forum **21** (2002) 149–172
6. Bernardini, F., Rushmeier, H.E., Martin, I.M., Mittleman, J., Taubin, G.: Building a digital model of michelangelo's florentine pietà. IEEE Computer Graphics and Applications **22** (2002) 59–67
7. Rusinkiewicz, S., Hall-Holt, O.A., Levoy, M.: Real-time 3d model acquisition. In: SIGGRAPH. (2002) 438–446
8. Coqueugniot, H., Couture, C., Dutailly, B., Gueorguieva, S., Desbarats, P., Synave, R.: Range image processing for paleoanthropology heritage preservation. In: DMAMH'2007, Proc. of the 2nd IEEE International Workshop on Digital Media and Its Applications in Museum and Heritages, DMAMH'2007, Chongqing, Chine, December 10-12. (2007)
9. Requicha, A.: Representation for rigid solids: Theory, methods and systems. ACM Computing Surveys (1980) 437–464
10. Requicha, A., Rossignac, J.: Solid modelling and beyond. IEEE Computer Graphics & Applications (1992) 31–44
11. Requicha, A.: Geometric Modeling: A First Course. Copyright 1996 The University of Southern California (1999)
12. Mortenson, M.: Geometric Modeling. John Wiley & Sons (1985)
13. Faux, I., Pratt, M.: Computational Geometry for Design and Manufacture. Ellis Horwood (1979)
14. Farin, G.: Gurves and Surfaces for Computer Aided Design. Academic Press (1988)
15. Fomenko, A., S.V.Mateev: Algorithms and Computer Methods for Three-Manifolds. Kluwer Academic Publishers (1997)
16. Farin, G., Hoschek, J., Kim, M.S.: Handbook of Computer Aided Design. North-Holland (2002)
17. Agoston, M.: Computer graphics and geometric modeling: mathematics. Springer (2005)
18. Agoston, M.: Computer graphics and geometric modeling: implementation and algorithms. Springer (2005)
19. Coxeter, H., Greitzer, S.: Geometry revisited. Mathematical Assocoation of America (1967)
20. O'Rourke, J.: Computational geometry in C (2nd edition). Cambridge university press (2001)
21. Hoffmann, C.: Geometric and Solid Modeling: An Introduction. Morgan Kaufmann (1989)
22. Szilvasi-Nagy, M.: Analysis of stl files. Mathematical and Computer Modeling (2003) 945–960
23. Curless, B., Levoy, M.: A volumetric method for building complex models from range images. In: SIGGRAPH '96: Proceedings of the 23rd annual conference on Computer graphics and interactive techniques, New York, NY, USA, ACM Press (1996) 303–312
24. Jaeggli, T., Koninckx, T.P., Gool, L.V.: Online 3d acquisition and model integration (2003)
25. Pauly, M., Mitra, N.J., Giesen, J., Gross, M.H., Guibas, L.J.: Example-based 3d scan completion. In: Symposium on Geometry Processing. (2005) 23–32
26. Synave, R., Desbarats, P., Gueorguieva, S.: Toolkit for registration and evaluation for 3d laser scanner acquisition. In: WSCG'2008, Proc. of the 16th International Conference in Central Europe on Computer Graphics, Visualisation and Computer Vision'2008, Plzen, Czech Republic. (2008) 199–204
27. Synave, R.: Reconstruction de solides à partir d'acquisitions surfaciques. PhD thesis, Université de Bordeaux1 (2009)
28. Besl, P.J., McKay, N.D.: A method for registration of 3-d shapes. IEEE Trans. Pattern Anal. Mach. Intell. **14** (1992) 239–256
29. Trucco, E., Fusiello, A., Roberto, V.: Robust motion and correspondence of noisy 3-d point sets with missing data. Pattern Recognition Letters **20** (1999) 889–898
30. Rusinkiewicz, S., Levoy, M.: Efficient variants of the icp algorithm. In: 3DIM. (2001) 145–152
31. Tsakiri, M., Ioannidis, C., Carty, A.: Laser scanning issues for the geometrical recording of complex statue. In: Optical 3D Measurement Techniques VI, Zurich. (2003) 214–222
32. Chetverikov, D., Stepanov, D., Krsek, P.: Robust euclidean alignment of 3d point sets: the trimmed iterative closest point algorithm. Image Vision Comput. **23** (2005) 299–309

33. Synave, R., Desbarats, P., Gueorguieva, S.: Automated trimmed iterative closest point algorithm. In: ISVC07, Proc of the 3rd International Symposium on Visual Computing, Lake Tahoe, Nevada, California, November, 26-28. (2007)
34. Bernardini, F., Mittleman, J., Rushmeier, H.E., Silva, C.T., Taubin, G.: The ball-pivoting algorithm for surface reconstruction. IEEE Trans. Vis. Comput. Graph. **5** (1999) 349–359
35. Allen, B., Curless, B., Popovic, Z.: The space of human body shapes: reconstruction and parameterization from range scans. ACM Trans. Graph. **22** (2003) 587–594
36. Nehab, D., Rusinkiewicz, S., Davis, J., Ramamoorthi, R.: Efficiently combining positions and normals for precise 3d geometry. ACM Trans. Graph. **24** (2005) 536–543
37. Samet, H.: Foundations of multidimensional and metric data structures. Morgan Kaufmann publishers (2006)
38. Guibas, L., Stolfi, J.: Primitives for the manipulation of general subdivisions and the computation of voronoi diagrams. ACM Transactions on Graphics **4** (1985) 74–123
39. Baumgart, B.: A polyhedron representation for computer vision. In: National Computer Conference. (1975) 589–596
40. Braid, I.: The sythesis of solids bounded by many faces. Communications of the ACM **18** (1975) 209–216
41. Mäntylä, M.: Geometric and Solid Modeling: An introduction. Computer Science Press (1988)
42. Shewchuk, J.R.: What is good linear element? interpolation, conditioning, and quality measures (2002)
43. Pébay, P.P., Baker, T.J.: Analysis of triangle quality measures. Math. Comput. **72** (2003) 1817–1839
44. Cabello, J.: Toward quality surface meshing. In: International Meshing Round Table. (2003) 201–213
45. Knupp, P.M.: Remarks on mesh quality (2007)
46. Botsch, M., Kobbelt, L.: A robust procedure to eliminate degenerate faces from triangle meshes. In: Visual Modeling and Visualization. (2001) 283–290
47. Bischoff, S., Kobbelt, L.: Towards robust broadcasting of geometry data. Computers & Graphics **26** (2002) 665–675
48. Yap, C.K.: Towards exact geometric computation. Comput. Geom. **7** (1997) 3–23
49. Yap, C., Mehlhorn, K.: Towards robust geometric computation. In: Fundamentals of computer science study conference. (2001) 214–222
50. Yap, C.K., Pion, S.: Special issue on robust geometric algorithms and their implementations. Comput. Geom. **33** (2006) 1–2
51. Mehlhorn, K., Yap, C.: Robust Geometric Computation. under preparation, http://www.cs.nyu.edu/cs/faculty/yap/book/egc/ (2004)
52. Kettner, L., Mehlhorn, K., Pion, S., Schirra, S., Yap, C.K.: Classroom examples of robustness problems in geometric computations. Comput. Geom. **40** (2008) 61–78
53. Karamcheti, V., Li, C., Pechtchanski, I., Yap, C.K.: A core library for robust numeric and geometric computation. In: Symposium on Computational Geometry. (1999) 351–359
54. Li, C., Yap, Ch. Pion, S., Du, Z., Sharma, V.: Core library tutoroal. In: Courant Institute of Mathematical Sciences, New York University. (2003) 1–46
55. Mehlhorn, K., Näher, S.: LEDA. Cambridge university press (1999)
56. Alexandroff, P.: Elementary Concepts of Topology. Dover,Inc. (1961)
57. Henle, M.: A Combinatorial Introduction to Topoly. Herman, Paris (1979)
58. Kinsey, L.: Topology of surfaces. Springer Verlag (1993)
59. Mitchell, J., Mount, D., Papadimitriou, C.: The discrete geodesic problem. SIAM J. Comput. **16** (1987) 647–668
60. Kimmel, R., Sethian, J.: Computing geodesic paths on manifolds (1998)
61. Chen, J., Han, Y.: Shortest paths on a polyhedron; part i: computing shortest paths (1996)
62. Kanai, T., Suzuki, H.: Approximate shortest path on a polyhedral surface and its applications. Computer-Aided Design **33** (2001) 801–811
63. Novotni, M., Klein, R.: Computing geodesic paths on triangular meshes. In: WSCG. (2002) 341–348
64. Martinez, D., Velho, L., Carvalho, P.: Computing geodesics on triangular meshes. Computers&Graphics **29** (2005) 667–675
65. Surazhsky, V., Surazhsky, T., Kirsanov, D., Gortler, S., Hoppe, H.: Fast exact and approximate geodesics on meshes. ACM Trans. Graph. **24** (2005) 553–560
66. Polthier, K., Schmies, M.: Straightest geodesics on polyhedral surfaces. In: SIGGRAPH '06: ACM SIGGRAPH 2006 Courses, New York, NY, USA, ACM (2006) 30–38
67. Lee, S., Han, J., Lee, H.: Straightest paths on meshes by cutting planes. In: 4th International Conference on Geometric modeling and processing. (2006) 609–615

68. Synave, R., Gueorguieva, S., Desbarats, P.: Constraint shortest path computation on polyhedral surfaces. In: ICVGIP'08, Proc. of the 6th Indian Conference on Computer Vision, Graphics and Image Pro cessing. (2008)
69. Polthier, K.: Polyhedral surfaces of constant mean curvature (2002)
70. Garimella, R.V., Swartz, B.K.: Curvature estimation for unstructured triangulations of surfaces. Technical Report LA-UR-03-8240, Los Alamos National Laboratory (2003)
71. Surazhsky, T., Magid, E., Soldea, O., Elber, G., Rivlin, E.: A comparison of gaussian and mean curvatures estimation methods on triangular meshes. In: ICRA. (2003) 1021–1026
72. Garland, M.: Notes on differential geometry (2004)
73. Blanchette, J., Summerfield, M.: C++ GUI programming with Qt4. Trolltech S.A. (2006)
74. Krause, A.: Foundations of GTK+ Development. Apress (2007)
75. Wood, B., Aiello, L., Wood, C., Key, C.: A technique for establishing the identity of "isolated" fossil hominin limb bones. Journal of Anatomy **193** (1998) 61–72
76. R., M., Saller, K.: Lehrbuch der Anthropologie. Bd 1 Fischer G Verlag, Stuttgart (1957)
77. Scheuer, L., Black, S.: The development of juvenile osteology. Academic Press (2000)
78. De la Villetanet, B.: Utilisation d'outils de mesures en 3d dans le cadre d'une etude comparative morphofonctionnelle de tali d'hominoides actuel et du hominide fossile. Technical Report Octobre, Univ. Bordeaux I, MS,spécialité anthropologie (2005)
79. Slice, D.: Modern morphometrics in physical anthropology. Kluwer academic plenum publishers (2005)
80. Allard, T., Sitchon, M., Sawatzky, R., Hoppa, R.: Use of hand-held laser scanning and 3d printing for creation of a museum exhibit. In: 6th International Symposium on Virtual Reality, Archaelogy and Cu ltural Heritage. (2005)
81. Gill-Robinson, H., Elias, J., Bender, F., Allard, T., Hoppa, R.: Using image analysis software to create a physical skull model for the facial reconstruction of a wrapped akhmimic mummy. Journal of computing and information technology **14** (2006) 45–51
82. Seulin, R., Stolz, C., Fofi, D., Millon, G., Nicolier, F.: 3d tools for ancient wooden stamps analysis and conservation. The Imaging Science Journal **54** (2006) 111–121
83. Carter, Y., Allard, T., Collin Moore, N., Goertzen, A., Klonisch, T., Hoppa, D.: The role of printing in teaching and education in human skeletal anatomy. The Journal of the Federation of American Societies for Experimental Biology **23** (2009)
84. Rossignac, J., Requicha, A.A.G.: Offsetting operations in solid modelling. Computer Aided Geometric Design **3** (1986) 129–148
85. Lee, S.H.: Offsetting operations on non-manifold boundary representation models with simple geometry. In: Symposium on Solid Modeling and Applications. (1999) 42–53
86. Maekawa, T.: An overview of offset curves and surfaces. Computer-Aided Design **31** (1999) 165–173
87. Chen, Y., Wang, H., Rosen, D.W., Rossignac, J.: A point-based offsetting method of polygonal meshes (2005)
88. Park, S.C.: Hollowing objects with uniform wall thickness. Computer-Aided Design **37** (2005) 451–460
89. Lee, S.H.: Offsetting operations on non-manifold topological models. Comput. Aided Des. **41** (2009) 830–846
90. Nizam, A., Gopal, R., Naing, L., Hakim, A., Samsudin, A.: Dimesional accuracy of the skull models produced by rapid prototyping technology using stereolithography apparatus. Archives of Orofacial Sciences 2006 (2006) 60–66